

## CAVITATION AND FRACTURE OF SOFT ADHESIVES

C. CRETON<sup>1</sup>, A. CHICHE<sup>1</sup>, J. DOLLHOFER<sup>1</sup>, A. ROOS<sup>1</sup>, C.Y. HUI<sup>2</sup>, V. MURALIDHARAN<sup>2</sup>

<sup>1</sup>Laboratoire de Physico-Chimie des Polymères et Milieux Dispersés, ESPCI, 10, Rue Vauquelin, 75005 Paris, France

<sup>2</sup>Department of Theoretical and Applied Mechanics, Cornell University, Ithaca NY 14853, USA

### ABSTRACT

Soft adhesives, are polymer based materials which stick upon the application of a light pressure. Because failure of these adhesives requires large deformations and linear and nonlinear viscoelasticity, quantitative modelling of their properties is difficult. We conducted extensive and detailed experimental investigations combining a customized probe test of confined layers of model soft adhesives with in-situ optical observation of the deformation mechanisms, to develop a micromechanical model of the failure processes of the adhesive bond. Failure is always initiated by the formation of cavities from initial germs, typically found at the interface between the adhesive film and the probe. For softer hyperelastic materials, the role of surface tension cannot be neglected and we find that cavitation occurs at values of stress distinctly higher than the elastic modulus  $E$ , and depending not only on the size distribution of the population of initial germs of cavities, but also on the thickness of the confined layer[1]. In light of our results we have then revisited cavity growth models to develop a possible description of the nucleation and growth of cavities adapted to very soft hyperelastic materials such as pressure-sensitive-adhesives, but also applicable to polymeric or biological highly swollen gels[2].

Once failure is initiated by the formation of cavities, the polymer can orient progressively in the direction of the tensile stress and form so-called fibrils. We have shown that these fibrils can store energy during the extension stage and subsequently rapidly release it when the fibrils break or are detached from the surface[3]. We have investigated these failure mechanisms with a series of block copolymer blends which form physically crosslinked networks. Depending on the diblock/triblock ratio in the blend, the extent of bridging molecules between domains vary and we found a profound effect of this extent of bridging on the nonlinear elastic and on the viscoelastic properties of the blends, which in turn affect fracture properties.

### 1 INTRODUCTION

Despite significant industrial interest in the topic, the criteria triggering fracture of soft materials, as commonly encountered in many applications such as self-adhesive products, cosmetics or biological tissues, have remained much more elusive than in the case of brittle solids. In brittle solids the common view of failure is that the material has intrinsic flaws. Failure in a structure occurs by the growth of one of these flaws into a crack which propagates catastrophically. In this picture, only the largest flaw matters since it will propagate catastrophically and the criterion for propagation is that of a critical energy.

In soft materials of course intrinsic flaws exist as well, however their growth under an applied remote stress does not necessarily lead to a catastrophic failure of the material. The propagation of a single crack accompanied by the release of elastic energy is seldom observed. Failure occurs more often by a mechanism more analogous to tearing, where highly dissipative processes involving large scale deformations of the material occur. These processes invariably involve, locally, the formation of cavities and the orientation and extension of polymer chains, reinforcing dramatically the resistance to fracture. Although a complete understanding of the failure process is difficult because it involves large deformations and linear and nonlinear viscoelasticity, the problem can be broken down into simpler ones. We have focused on two aspects of the fracture

process: the criteria controlling the formation of cavities in a soft material, and the formation and growth of the oriented fibril structure.

## 2 EXPERIMENTAL METHODS AND MATERIALS

### 2.1 Adhesive films

We performed the entire study with model pressure-sensitive-adhesives, namely blends of a symmetric styrene-isoprene-styrene triblock copolymer (SIS), an asymmetric SI block copolymer and a hydrogenated resin miscible with the isoprene. Due to the immiscibility between styrene and isoprene, the PS end-blocks form rigid nodules that act as physical crosslink points for the melt isoprene chains[4]. The resulting material is a soft physically crosslinked rubber with a low storage elastic modulus ( $E' \sim 0.2$  MPa) and a relatively low loss modulus ( $E'' \sim 0.02$  MPa at 0.1 rad/s). Films with different compositions (0,19,42 and 54% diblock), 60% resin and with different dry thicknesses were cast: 60  $\mu\text{m}$ , 120  $\mu\text{m}$  and 240  $\mu\text{m}$ , by using different concentrations of the SIS + resin blend (respectively 7.5 wt%, 15 wt% and 30 wt%).

### 2.2 Probe tests

The probe tests that we performed and the homemade setup we used have been extensively described elsewhere[5, 6]. First, the flat end of the probe is brought in contact with the adhesive layer that is on a transparent rigid substrate. When the desired contact pressure is reached, the probe is kept motionless for one second before being separated at a constant probe velocity  $V$ . The force  $F$  (compression then tension) and the film thickness  $h$  (distance between the probe surface and the film substrate) are monitored, and the images of the contact area are taken through the transparent film substrate using a microscope. The probe we used consists of a flat-ended cylinder made of stainless steel (radius = 3 mm).

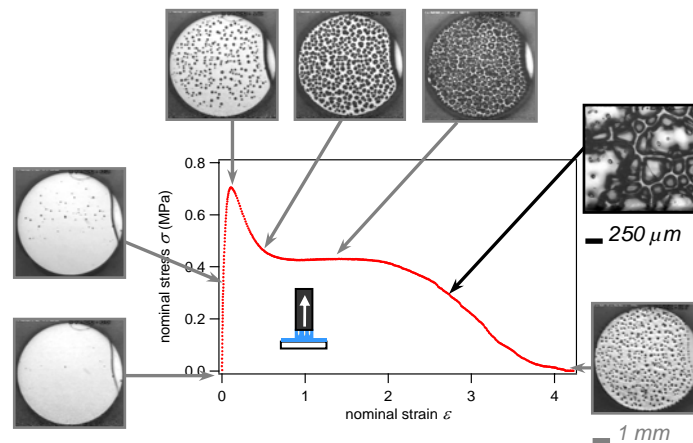


**Figure 1.** Typical nominal stress versus nominal strain, and optical images of the contact (taken through the transparent adherent) at different debonding times.

We used in this study two different surface treatments for the flat end which makes the contact with the adhesive film. The two probes are polished with two different abrasive papers in order to get different levels of surface roughness. The surfaces are named "rough" and "smooth" for convenience. The RMS degree of roughness was of 10 nm and 150 nm respectively[7].

The contact area  $A_0$  at the beginning of the pull-off stage is measured from the images, and we use this value to convert the force  $F$  to a nominal stress  $\sigma$  ( $\sigma=F/A_0$ ). We also convert the film thickness  $h$  into a nominal deformation  $\varepsilon$  using the initial thickness  $h_0$  ( $\varepsilon=h-h_0/h_0$ ). This way, a nominal stress versus strain curve can be represented (figure 1).

The images of the contact show that for this kind of permanent adhesive cavities appear and grow all over the surface of the contact. At the bottom of the first peak, the adhesive film resembles a foam. The final plateau in nominal stress is related to the stretching of the resulting bi-dimensional foam. In this study we focus on two regions of the force-displacement curve: the initial peak, related to the cavitation process, and the plateau of stress after the peak, which is related to the extension of the fibrils.

### 3 RESULTS

#### 3.1 Cavity growth

The effect of the adhesive film thickness  $h_0$  on the cavitation process (through the first peak stress  $\sigma_{max}$ ) is shown in Figure 2. If the surface of the probe is rough, the maximal stress does not vary with the adhesive film thickness. This result is compatible with a critical stress criterion for the cavitation mechanism ( $\sigma_{cav} \sim E'$ )[8]. In the case of a smooth adhesive and smooth probe surface, however,  $\sigma_{max}$  decreases as the adhesive film thickness increases.

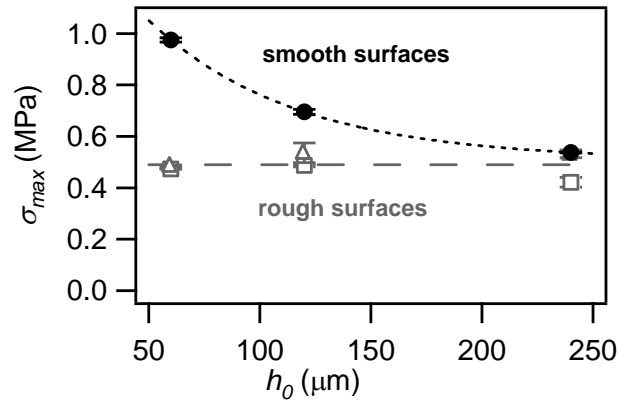


**Figure 2.** Variations of the maximum nominal stress  $\sigma_{max}$  during the adhesive separation (associated with the cavitation process) with the adhesive layer thickness  $h_0$ . The full black symbols correspond to the smooth adherent surface, and the open symbols to the case of large interfacial defects.

In this case in fact, the elastic energy stored in the adhesive film during the initial tensile stage, i.e. from the beginning of the debonding ( $\sigma = 0$ ) to the development of the cavities ( $\sigma_{max}$ ), is almost constant regardless of the adhesive film thickness. The cavitation mechanism appears then to be triggered by an energy criterion  $W_{cav} \sim 7 \text{ J.m}^{-2}$ .

Cavitation starts from initial germs formed during the imperfect contact between the layer and the probe. If these germs are large enough, all cavities grow simultaneously during the debonding

as a function of the applied stress. Their growth rate does not depend on their size, since the stress criterion is almost the same (Figure 2) for a range of initial (large) germ sizes[1].

If the initial germs are not large enough (smooth adhesive and adherent case), the cavities appear sequentially during the debonding, and grow at different rates depending when they appear. If they appear at low levels of stress, the growth rate is slow and resembles that of cavities growing from large defects. However when the cavity appears later in the experiment, i.e. at higher levels of stress, it can grow much faster. As pointed out earlier, the cavitation appears to be controlled by a critical stored energy in the layer criterion, more than a by a critical stress criterion in the case of small initial germs.

This sensitivity to the initial germ size is a consequence of the surface energy that needs to be created for a cavity to grow. Based on the assumption that potential flaw-size effects could result from the incorporation of surface energy  $\gamma$ , the model of cavitation that we developed is able to predict such a transition from a stress criterion for large flaws to an energy criterion for small flaws and details are given in a recently published paper[2]. The limit between these two regimes of small and large initial flaws is given by the ratio  $\gamma/E'$ . For the typical PSA we used in this study ( $E' = 0.2$  MPa and  $\gamma = 30$  mJ/m<sup>2</sup>), the critical initial flaw size  $r_0$  that the model predicts is around 150 nm, in very good agreement with our experiments[1]. The thickness dependence of the measured value of  $\sigma_{\max}$  is more difficult to predict simply from the introduction of surface tension. We believe that this new and somewhat surprising result can be interpreted with a model for the growth of small germs in finite size layers. This model is mainly based on the dual notion of an energy activated transition from an unexpanded metastable state to an expanded stable state and to the proportionality of the activation energy with the elastic energy stored in the adhesive layer[2].

Although this interpretation is consistent with experimental results, it is important to recognize that the layer thickness where the stress overshoot is no longer observed is three orders of magnitude larger than the critical defect size, implying somehow that the growing defect can draw elastic energy from a volume up to a 1000 times larger than its own size. It is not easy to envision where this extreme sensitivity could come from and further experiments performed with different materials having a range of elastic moduli, and with different experimental geometries, should shed more light on the exact mechanism triggering cavity growth.

### 3.2 fibril formation and growth

Once all cavities are nucleated, the walls between cavities extend in the direction of the applied tensile stress, forming effectively an elongated structure of cavity walls, often called fibrillar structure. This structure does not vary much with adhesive composition. However the large strain part of the stress-strain curve, and therefore the mechanical properties of the walls, is significantly affected by the diblock/triblock ratio as can be seen on figure 3[3, 9]. The adhesive made with pure triblock has the highest plateau stress while, an increase in diblock content causes the fibril extension to occur at lower stresses but detach at higher extensions.

Since it is often assumed that adhesive properties are controlled by the rheological properties for soft adhesives, we measured the dynamic shear modulus  $G'$  of each PSA at a frequency approximately equivalent to the initial strain rate applied to the layer. However, at a strain rate of 1 s<sup>-1</sup>, all adhesives are roughly equivalent in terms of shear modulus, failing therefore to account for the differences observed on figure 3. The reason for this failure is that in this regime, the response of the adhesive is very dependent on its *non-linear elastic* properties. When the triblock in the formulation is replaced by two diblocks, the linear viscoelastic properties are not much affected (and only at low frequency) but the nonlinear elastic properties are very affected as shown on figure 4.

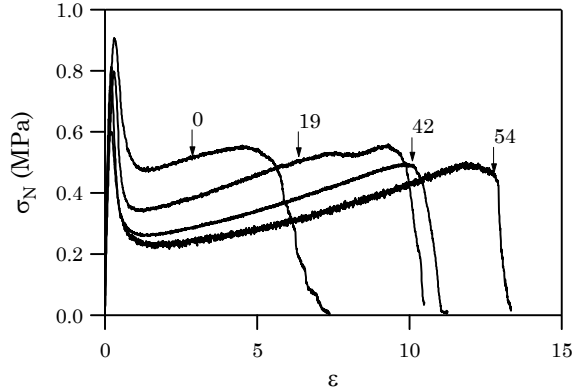


**Figure 3:** Probe tack curves of a series of block copolymer based adhesives. The probe velocity is the same ( $100 \mu\text{m/s}$  corresponding to an initial strain rate of  $1 \text{ s}^{-1}$ ) and the number refers to the proportion of diblock in the blend.

Phenomenologically, the initial portion of the nominal stress ( $F/A_0$ ) vs.  $\lambda$  curve (up to  $\lambda = 5$ ) can be well represented by a Mooney-Rivlin constitutive equation of the type:

$$\sigma_N = 2 \left( C_1 + \frac{C_2}{\lambda} \right) \left( \lambda - \frac{1}{\lambda^2} \right) \quad (1)$$

with  $C_1 \ll C_2$ . Physically this behavior can also be modeled by a molecularly based rubber elasticity model, taking into account both entanglements (which dominate the behavior at low strains) and crosslinks (which dominate the behavior at high strains). Since for our adhesives, the density of entanglements is significantly larger relative to the density of physical crosslinks, the effect of the crosslink density is only visible at high strains. It is interesting to examine figure 4 more closely. The nominal stress is a good way to represent the overall force applied on the adhesive and is directly comparable to the stress measured in figure 3 in the probe tests. In that representation, the pronounced softening of the material around 100% strain bears a striking resemblance to the yield stress of a glassy or semi-crystalline polymer. The effect of this softening at large strains, will be to prevent crack propagation by favoring crack blunting, and to favor the formation of highly extended fibril structures, under a nearly constant force.

The importance of this result becomes apparent when relaxation experiments are performed. Probe tests can be carried out classically by pulling the probe at a constant velocity until complete detachment of the adhesive from the probe occurs. However it is also possible to stop the test while the fibrillar structure has been formed, but is not yet detached from the probe. If the force in the fibrils were essentially due to viscous dissipation, the force would then quickly relax to zero. However these experiments, shown on figure 5 for a representative adhesive, show conclusively that the force does not relax to zero but only to a limiting value, demonstrating therefore the elastic character of the fibrils. In essence the fibrillar structure acts as an energy reservoir, and stores elastic energy, which is then suddenly dissipated upon detachment of the fibrils.

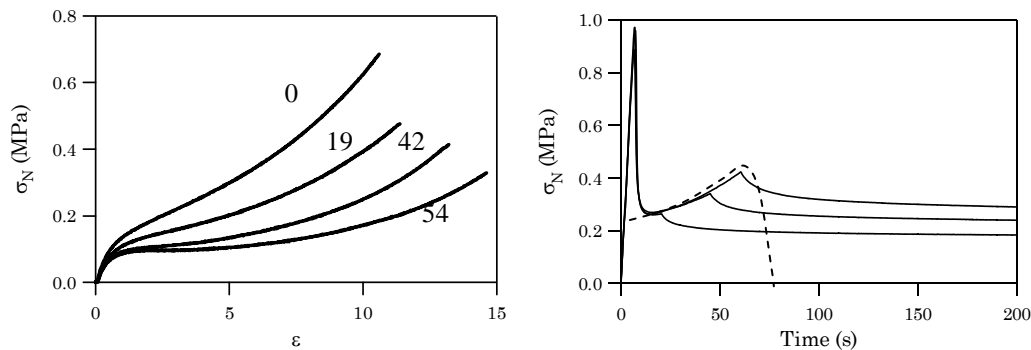


**Figure 4:** Stress-strain curves in uniaxial elongation of the same adhesives tested in probe tack on figure 1. Data from [3].

**Figure 5:** Nominal stress vs. time curves with displacement stops: 600 s stops at the beginning, the middle and the end of the fibrillation process, compared to a debonding curve without stop(dashed line).

#### 4 CONCLUDING REMARKS

We have investigated the fracture mechanisms of interfaces between soft hyperelastic layers (modulus  $< 0.1$  MPa) and a rigid surface. Fracture is always initiated by the formation of cavities nucleated at the interface, but growing in the bulk of the layer. Cavities grow from existing germs of various sizes which are created by the surface topography. For germs larger than  $\gamma/E$ , the growth of a germ to a macroscopic cavity occurs at a given stress level which only depends on the nonlinear elastic properties of the adhesive. For germs smaller than  $\gamma/E$ , growth occurs at a stress level which depends both on germ size and on layer thickness strongly suggesting that a necessary condition for expansion of the cavity is a sufficient amount of energy stored in the layer. Once all the cavities are formed, the adhesive layer becomes a foam and the walls between cavities progressively orient in the direction of traction to form a nearly elastic fibrillar structure. The amount of elastic energy that can be stored in this structure is controlled by the nonlinear elastic properties of the adhesive.

#### 5 REFERENCES

- [1] Chiche, A., Dollhofer, J. and Creton, C., submitted to Eur. Phys. J. E
- [2] Dollhofer, J., Chiche, A., Muralidharan, V., Creton, C. and Hui, C. Y., *Int. J. Solids Structures*, 41, 6111-6127, (2004)
- [3] Roos, A., 2004, Ph. D. thesis, Université Paris VI.
- [4] Daoulas, K., Theodorou, D. N., Roos, A. and Creton, C., *Macromolecules*, 37, 5093-5109, (2004)
- [5] Lakrout, H., Sergot, P. and Creton, C., *J. Adhes.*, 69, 307-359, (1999)
- [6] Josse, G., Sergot, P., Dorget, M. and Creton, C., *J. Adhes.*, 80, 87-118, (2004)
- [7] Chiche, A., Pareige, P. and Creton, C., *C.R. Acad.Sci. Paris, IV*, 1, 1197-1204, (2000)
- [8] Gent, A. N. and Lindley, P. B., *Proc. Roy. Soc. London, A*, 249 A, 195-205, (1958)
- [9] Roos, A. and Creton, C., *Macromol. Symp.*, 214, 147-156, (2004)